Chemical Physics 136 (1989) 429–442
North-Holland, Amsterdam

LINE-NARROWING SPECTROSCOPY IN AMORPHOUS SOLIDS THROUGH POLARIZATION DETECTION OF SPECTRAL HOLES. II. APPLICATION TO TETRAPHENYLPORPHIN IN PMMA

Bernhard DICK
Max-Planck-Institut für biophysikalische Chemie, Abteilung Laserphysik, D-3400 Göttingen, FRG

Received 11 April 1989

Polarization spectroscopy of photochemically produced spectral holes has been used to obtain the line-narrowed spectrum of the first electronic transition of meso-tetraphenylporphin (TPP) in a PMMA matrix at 10 K. The spectral holes have been burned through irradiation with a pulsed dye laser into the spectral region of several vibronic transitions with overlapping inhomogeneous bands. The corresponding satellite holes were detected in the spectral region of the electronic origin. More than 50 lines have been observed up to vibrational wavenumbers of 1850 cm^{-1} above the electronic origin. The inhomogeneously broadened absorption spectrum displays only two broad bands in this spectral region. The vibrational frequencies of the first excited electronic state of TPP obtained in this way agree very well with those obtained for the same molecule with fluorescence spectroscopy in a supersonic jet, in a polystyrene matrix, and a crystalline Shpol'skii host. They are also very similar to those of the electronic ground state known from resonance Raman spectra. An analysis of the linewidths of resonant holes and satellite holes reveals a small effect of the inhomogeneous site distribution on the vibrational frequencies.

1. Introduction

In the preceding paper [1] we have proposed a combination of spectral hole-burning with polarization spectroscopy as a new method to obtain line-narrowed spectra of molecules in amorphous environments. Spectral hole-burning with laser light of frequency ω_B is used to selectively excite a homogeneously broadened subensemble of molecules and remove it from the inhomogeneously distributed total ensemble. In this way the absorption spectrum of these hole-burned molecules is removed from the total absorption spectrum. For each vibronic transition of the molecule a spectral hole is produced which can be detected as a small increase ΔI of transmission of a probe light beam which had transmission I_0 before hole-burning. The contrast ratio $\Delta I/I_0$ of the spectral holes is usually very small and suffers from serious signal-to-noise problems, especially when a pulsed laser is used for probing.

This contrast ratio can be dramatically improved through the use of polarization spectroscopy [2]. Hole-burning with polarized light will produce a hole in the orientational distribution of molecules in addition to the spectral hole. When the transmission spectrum is taken with the sample between a pair of crossed polarizer and analyzer, the isotropically oriented subensembles will not contribute to the signal. Through slight detuning of the polarizer from perfect crossing with the analyzer a background light field can be intentionally mixed with the signal light field yielding additional information on the relative orientation of transition dipole moments in the molecule.

In the present paper we apply this method to the line-narrowing spectroscopy of meso-tetraphenylporphin (TPP) in polymethylmethacrylate (PMMA) matrix. This molecule was chosen as a first example for the following reasons:

(1) Porphins are well known for photochemical hole-burning following excitation to the first excited singlet state. The first absorption band is in the visible spectral region and easily accessible with dye lasers.

(2) TPP is readily available and comparatively stable against oxygen and light.

(3) The vibrational frequencies of TPP in its first excited singlet state have been studied with fluores-

0301-0104/89/$ 03.50

cence excitation techniques in an amorphous host (polystyrene) [3], in a crystalline Shpol'skii matrix (nitrobenzene) [4], and for the isolated molecule in a supersonic jet [5]. Thus several sets of data exist for comparison.

We define the polarization hole-burning spectrum $S(\omega)$ as the transmission spectrum obtained with nearly crossed polarizer and analyzer, I_{AP}, normalized to the transmission spectrum obtained with the analyzer parallel to the polarizer, I_{PP}. For a single spectral hole produced by hole-burning into the transition $|a\rangle \rightarrow |b\rangle$ and probing of the transition $|a\rangle \rightarrow |c\rangle$ the expected lineshape is

$$S(\omega) = \frac{I_{AP}}{I_{PP}} = \left| \frac{A_{abc}}{\omega - \omega_H - i\Gamma_{abc}} + iB \right|^2 . \qquad (1)$$

This is a Lorentzian lineshape centered at $\omega_H = \omega_B + \omega^0_{cb}$, where ω_B is the frequency of the laser used for hole-burning, and $\omega^0_{cb} = (E_c - E_b)/\hbar$ is the transition frequency of the transition $|b\rangle \rightarrow |c\rangle$. In the present paper this will always be a vibrational transition within the first excited electronic singlet state of TPP. In deriving eq. (1) the contribution of the phonon wings of the molecular transitions and the spectral width of the light sources have been neglected. It was further assumed that the inhomogeneous width of the absorption band is much larger than the homogeneous widths, that the photoreaction was not saturated, and that the inhomogeneous distribution for the hole-burned transition is perfectly correlated with the inhomogeneous distribution of the probed transition. This means that a constant value of ω^0_{cb} is assumed for all molecules. (More general situations including phonon wings and imperfect correlation will be treated in a separate theoretical paper [6].) The parameters A, B, and Γ have been discussed in ref. [1]. Briefly, they have the following meaning:

B is proportional to the scalar product $e_A \cdot e_P$ of the unit vectors indicating the orientation of the polarizer and analyzer. It represents the intentionally admixed background field. With perfectly crossed polarizer and analyzer $B = 0$. Rotation of the polarizer towards the analyzer produces a positive background field, rotation into the opposite direction produces a negative background field.

Γ_{abc} is the sum $\Gamma_{ab} + \Gamma_{ac}$ of the phase-relaxation rate constants of the two molecular transitions. The width (fwhm) of a satellite hole is $B_H = 2\Gamma_{ab}$, that of a resonant hole ($|b\rangle = |c\rangle$) is $B_H = 4\Gamma_{ab}$. In the limit of perfect correlation between the inhomogeneous distributions the satellite hole has the mean width of the corresponding two resonant holes. In the case of less perfect correlation the complex Lorentzian in eq. (1) must be convoluted with the homogeneous distribution function for ω_{cb} leading to an increase of the linewidth [6]. The difference of the width of the satellite hole and the mean width of the two resonant holes is then a measure of the width of the inhomogeneous distribution of the vibrational frequency ω_{cb} [7].

A_{abc} is an amplitude factor containing the oscillator strengths of the two molecular transitions, the probability of finding a molecule with transition frequency $\omega_{ba} = \omega_B$ in the ensemble, the fluence of hole-burning light applied, and the factor $(\cos^2\theta - 1/3)$, where θ is the angle between the transition dipole moments of the transitions $|a\rangle \rightarrow |b\rangle$ and $|a\rangle \rightarrow |c\rangle$.

TPP has a center of symmetry [8] and is usually assigned to the point group D_{2h}. The transition dipole moment of the first electronic transition $S_0 \rightarrow S_1^x$ is along the x axis joining the two inner protons [9]. Vibronic transitions to the same electronic state involving totally symmetric vibrations (a_g symmetry) will have the same polarization. Hence satellite holes belonging to a_g vibrations will have an amplitude A with positive sign when either burning or probing of the hole is done with the electronic origin transition. Vibronic transitions involving in-plane vibrations of b_{1g} symmetry or out-of-plane vibrations of b_{2g} symmetry will be polarized along the y axis (in-plane) or z axis (out-of-plane), respectively. The corresponding satellite holes will have a negative amplitude when either burning or probing of the hole is done with the electronic origin transition. Such vibrations must borrow their intensity through Herzberg–Teller coupling to an electronic transition with a transition dipole in the y or z direction. Since the low-lying electronic singlet states of TPP including the strong Soret band at 418 nm are polarized in the molecular plane [10,11], the transition to vibronic states of S_1^x corresponding to out-of-plane vibrations should be very weak. Hence reasonably intense satellite holes with negative amplitude can be assigned to b_{1g} vibrations.

In realistic situations the inhomogeneous distributions of several transitions will overlap. Then eq.

(1) must be summed over all states $|b\rangle$ and $|c\rangle$ in question before taking the square modulus. When the inhomogeneously broadened absorption band of the electronic origin is well separated from the other bands, as is the case for TPP, two situations may be distinguished:

(1) A single hole is burned into the inhomogeneous distribution of the electronic origin band. The hole spectrum is scanned over the spectral region of the total absorption spectrum, yielding a hole for each vibronic transition [12]. This case was termed hole-burning of type-I satellites [1].

(2) Hole-burning into the spectral region of overlapping vibronic bands will produce many holes in the inhomogeneous ensemble, one for each vibronic state. These holes are scanned over the spectral region of the electronic origin band [13,14]. This case was termed hole-burning of type-II satellites [1].

In the present paper both situations have been studied. Type-II hole spectra were found to yield far better results in agreement with the theoretical considerations made earlier [1].

2. Experimental

2.1. Samples

Methylmethacrylate (MMA) was obtained from Merck and distilled twice under reduced pressure to remove the inhibitor and impurities. α, α′-azoisobutyronitrile (Aldrich) was used as supplied. Two different samples of meso-tetraphenylporphin (TPP) were used: one was obtained from EGA and contained about 3% of meso-tetraphenylchlorin [15], the other was obtained from Aldrich and was certified as chlorin-free. Both samples were used without further purification and yielded identical results.

In our previous experiment [2] we used polymethylmethacrylate (PMMA) films cast from a solution of TPP and a PMMA granulate in chloroform onto sapphire substrates. This method had several disadvantages: The commercially available granulates contain unknown impurities which can react with some guest molecules. E.g., Elvacit 2000 (Du Pont) released acid and produced the green protonated form of TPP. This could be avoided through washing the granulate with KOH in ethanol. Another guest molecule, 3-hydroxyflavone, was decomposed within minutes in a solution containing a PMMA granulate from Aldrich (low molecular weight, #18223-0). Since we found no way to remove these reactive impurities we decided to produce PMMA samples from the purified monomer. In this case the samples are also free of solvent. It has been found that residual solvents in polymer films can increase the width of spectral holes [16,17]. Also, some solvents like chloroform may cause photochemical reactions when irradiated with UV light.

The polymerization was carried out in 2 cm diameter glass tubes filled with 35 ml of a saturated solution of TPP in MMA and 12 mg of α,α′-azoisobutyronitrile as radical starter. The solution was degassed through four freeze–pump–thaw cycles and sealed off under vacuum. To avoid the formation of bubbles polymerization was initiated very slowly by keeping the tube at 40°C for at least 5 days. Subsequently the temperature was raised to 60°C (2–3 days) and 80°C (2–3 days). A final annealing at 125°C for one night followed by slow cooling to room temperature was found necessary to remove strain in the sample which otherwise resulted in strong birefringence. From the resulting PMMA slab thin slices were cut and optically polished on both sides. The final samples had thickness between 0.7–2.0 mm and an optical density of about 1.0 at the first absorption maximum of TPP at 648 nm at room temperature.

The sample had to be cooled by the cool finger of a closed-cycle refrigerator cryostat (Leybold ROK 300-10) solely through thermal conduction. Hence it had to be firmly attached with a large area onto a transparent substrate with good thermal conductivity. As substrate material LiF windows of 2 mm thickness were chosen to avoid the birefringence of sapphire.

Considerable difficulties were encountered when trying to establish good thermal contact between the sample and the substrate. It was not sufficient to press the sample against the LiF window with springs, or to mount it between two LiF windows. In most cases when the sample was glued to the LiF window the strong strain which developed during cooling caused breaking of the glue or the LiF window. The best results were obtained with silicon rubber glue (Wacker E41) which survived usually several cooling cycles without loss of the optical quality of the PMMA–LiF compound.

2.2. Experimental setup

The experimental setup has been described in detail in the preceding paper on the principles of the method [1]. The dye laser was operated with rhodamine 101, rhodamine B, and rhodamine 6G. Its bandwidth was less than 0.2 cm^{-1}. The intensity of all hole spectra given in this paper is the ratio of the intensity of the light transmitted through the analyzer, I_{AP}, and that rejected by the analyzer, I_{PP}. This ratio I_{AP}/I_{PP} was measured for each individual laser pulse and averaged over 20 events for each wavelength setting of the dye laser. The dye laser was scanned in steps of 0.21 Å unless otherwise noted in the figure caption. The intensity of the dye laser was varied with neutral density filters. Pulse energies for hole-burning ranged from 1 μJ/pulse (20 pulses) at 645 nm in the region of the electronic origin band of TPP up to 11 μJ/pulse (1000 pulses) at 580 nm in the vibronic band. For scanning of the spectra the laser was attenuated to about 20 nJ/pulse.

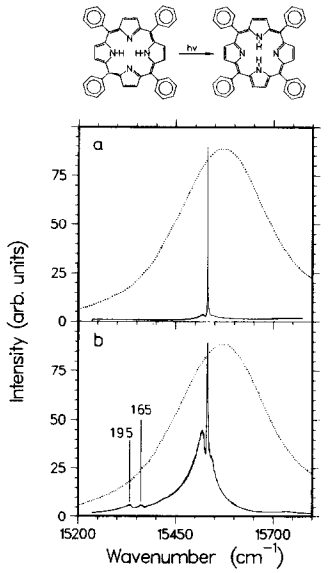

Fig. 1. Top: Structural formula of TPP and photochemical reaction leading to spectral hole-burning. Below: Polarization spectra of resonant spectral holes burned into the electronic band of TPP in PMMA at 10 K. Burning fluence was about 2.3 mJ/cm² in (a) and about 47 mJ/cm² in (b). The dotted line indicates the inhomogeneously broadened absorption band at 10 K.

3. Results

3.1. The resonant hole in the electronic origin band

Fig. 1 shows two hole spectra obtained after hole-burning into the origin band of the first electronic transition of TPP in PMMA. The inhomogeneously broadened absorption band of this transition is shown as dotted line. Spectrum (a) was observed with a hole-burning fluence of about 2.3 mJ/cm² and displays a sharp zero-phonon line. A fit of the complex Lorentzian lineshape function of eq. (1) yields a width of $2\Gamma = 0.99$ cm^{-1}. For spectrum (b) a much larger fluence of about 47 mJ/cm² was applied to the sample. The zero-phonon line is broadened to $2\Gamma = 3.0$ cm^{-1}, and is superimposed on a broad band with about 35 cm^{-1} width resulting from the excitation of phonon sidebands. This behavior indicates photochemical saturation due to strong depletion of those TPP molecules which have their zero-phonon line in resonance with the hole-burning frequency. In addition to the resonant hole in fig. 1b two weak satellites appear at 165 and 195 cm^{-1} red-shifted from the hole-burning frequency. These indicate two low-frequency vibrations of TPP whose Franck–Condon factors are much smaller than that of the electronic origin.

For a quantitative comparison of the lineshape of the hole with the theoretical expression of eq. (1) photochemical saturation of the hole must be avoided through application of only a low fluence. In fig. 2 a high-resolution scan of a resonant hole burned into the electronic origin of TPP is shown together with the best fit to eq. (1). The difference between both spectra is shown as curve (c) and indicates no systematic deviation. This indicates that the lineshape of the hole is indeed well described by eq. (1). The linewidth $2\Gamma = 0.98$ cm^{-1} of the hole can, however, not be interpreted as twice the homogeneous linewidth of the electronic origin of TPP in PMMA at 10 K. The reason is that high laser intensities can lead to broadening of the hole without affecting its Lorentzian shape. For free-base porphin this effect was observed with cw laser excitation with intensities of less than 1 mW/cm² [17]. With higher laser intensities this broadening reaches a saturation value. Thus the high peak intensity of the pulsed dye laser used in our

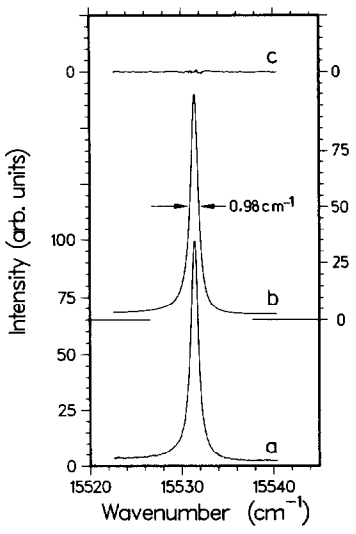

Fig. 2. (a) High-resolution polarization spectrum of a resonant hole burned into the electronic origin band of TPP at 10 K. The scan was performed in steps of 0.0315 Å. (b) Best fit of eq. (1) to the experimental spectrum with $\Gamma = 0.488$ cm^{-1}. (c) Difference between experimental spectrum and fit.

Table 1
Temperature dependence of spectral holes in the electronic origin band of TPP in PMMA observed through polarization spectroscopy. Amplitudes A and widths Γ were obtained through least-squares fits of eq. (1) to the experimental lineshapes. Note that the peak signal intensity scales with A^2/Γ^2

T (K)	A	Γ (cm^{-1})
10.0	1.00	0.55
11.5	0.74	0.55
13.5	0.39	0.58
15.2	0.19	0.64
17.6	0.02	0.63

investigation could be responsible for a considerable part of the observed hole width.

Repeated scans of a hole burned at 10 K showed that no significant change in the depth or width of the hole occurred over a time of several days. However, when the temperature was raised, the depth of the hole decreased drastically (see table 1). At 20 K the signal was less than 0.1% of that at 10 K and dropped to the noise level. This disappearance of the hole could be due to back-reaction of the protons in the TPP molecule, conformational relaxation of TPP, or relaxation of the surrounding PMMA chains causing a shift of the resonance frequency. The fact that after each increase of the temperature a fraction of the hole is filled may indicate a distribution of barriers for these relaxation processes. During heating of the sample the temperature inside the thin PMMA plate might temporarily reach values higher than the preset value. For a quantitative analysis a much more precise temperature regulation and better heat contact of the sample are required, preferably through cooling with He exchange gas[#1].

Interestingly the linewidths of the hole increased only slightly with rising temperature. If spectral diffusion is neglected, the expected linewidth of the hole is the sum of the homogeneous widths of the transition when it was burned and when it was probed. The first width is the homogeneous width at 10 K plus the contribution from intensity broadening mentioned above. The second is the homogeneous width at the probe temperature. From a $T^{1.3}$ dependence of the homogeneous width [18] an increase of the hole width by 70% is expected when the hole is probed at twice the temperature of hole-burning and no other broadening is present. The much smaller increase in the hole width observed must then be due to a large contribution of the intensity-broadening component. This broadening then sets a limit to the resolution achievable with pulsed dye lasers.

3.2. *Vibrational satellite holes of type I*

Whereas with moderate laser fluences very strong and sharp resonant holes could be produced in the electronic origin of TPP, the corresponding vibronic satellites were found to be very weak. In fig. 3 the hole spectrum after hole-burning with a fluence of about 28 mJ/cm^2 is shown. Although the resonant line is already saturated, indicated by the broad underlying contribution from the phonon sideband, even the strongest satellite holes have intensities less than 1% of the resonant hole. In addition a background with broad bands is produced, presumably due to the molecules burned into the phonon side-

[#1] The closed-cycle cryostat used for the present investigation is certainly not the optimum choice for these types of experiments. A liquid-helium cryostat provides a much lower base temperature, thus considerably reducing phonon sidebands. It also should give a much more homogeneous and stable temperature profile across the sample.

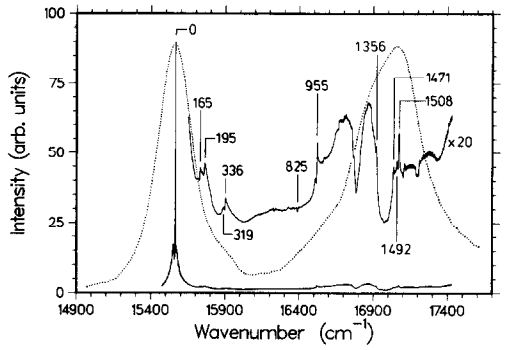

Fig. 3. Polarization spectrum of type-I satellite holes. Hole-burning was performed at $\nu_B = 15562\ cm^{-1}$ with a fluence of about 28 mJ/cm^2. The spectra were scanned in three sections with dyes rhodamine 101, rhodamine B, and rhodamine 6G. Satellite lines are labelled with their vibrational wavenumbers. The dotted line is the absorption spectrum of the sample at 10 K.

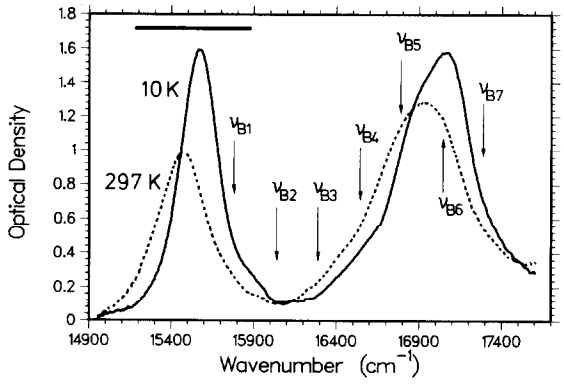

Fig. 4. Absorption spectrum of TPP in PMMA at room temperature (dotted line) and 10 K. The thickness of the sample was 2 mm. The wavenumbers of hole-burning are indicated with arrows and labelled ν_{B1}–ν_{B7}. The type-II satellite spectra were scanned over the range indicated by the horizontal bar.

band. For the vibrational zero-phonon lines these broad bands act like a complex background B in eq. (1), leading to dispersion-like shapes as for the line 955 cm^{-1} above the resonant hole. The small intensities of all satellite holes indicate that the Franck–Condon factors of all vibrations are much smaller than that of the origin. Nevertheless ten satellite lines could be reproducibly located.

3.3. Vibrational satellite holes of type II

The small Franck–Condon factors for all vibrations compared to that of the electronic origin suggest the applicability of the second type of hole-burning discussed in ref. [1], namely hole-burning into the vibronic state followed by detection in the spectral region of the electronic origin. In fig. 4 the absorption spectrum of TPP in PMMA in the region of the $S_0 \rightarrow S_1^v$ transition is shown for room temperature (dotted line) and 10 K (full line). Hole-burning experiments were performed at seven wavenumbers increasing with increments of 250 cm^{-1}. The spectral positions are indicated by arrows in fig. 4 and labelled ν_{B1} to ν_{B7}. In all experiments the polarization spectrum was scanned over the range indicated by the horizontal bar in fig. 4. The resulting spectra are shown in figs. 5–11. Each figure contains three spectra: one (a) obtained with the polarizer and analyzer perfectly crossed, one (b) with the polarizer rotated away from the analyzer, corresponding to a negative background field ($B<0$ in eq. (1)), and one (c) with the polarizer rotated towards the analyzer corresponding to a positive background field ($B>0$).

The spectra in fig. 5, obtained after hole-burning at $\nu_{B1} = 15782\ cm^{-1}$, show four satellite holes with vibrational wavenumbers of 165, 195, 319 and 336 cm^{-1}. The resonant hole appears also as a weak feature since the hole-burning frequency is still in the far wing of the inhomogeneous absorption band of the electronic origin indicated by the dotted line in fig. 5. A negative background produced through detuning of the polarizer away from the analyzer leads to inversion of all lines (see fig. 5b). All four satellite lines have positive amplitude factors A in eq. (1) indicating that the transition dipole moments of these vibronic transitions are parallel to the electronic transition moment. To check whether a line with negative amplitude factor is hidden in this spectral region, a scan with the polarizer detuned towards the analyzer was performed (fig. 5c), but with negative result.

Hole-burning at $\nu_{B2} = 16032\ cm^{-1}$ produces the spectra shown in fig. 6. The strongest feature is a line displaced 336 cm^{-1} from the hole-burning frequency. It corresponds to the line with the same shift seen in fig. 5, but appears now blue-shifted by 250 cm^{-1} at the high-energy side of the inhomogeneously broadened absorption band. The lines at displacements of 319 and 195 cm^{-1} are also found, although

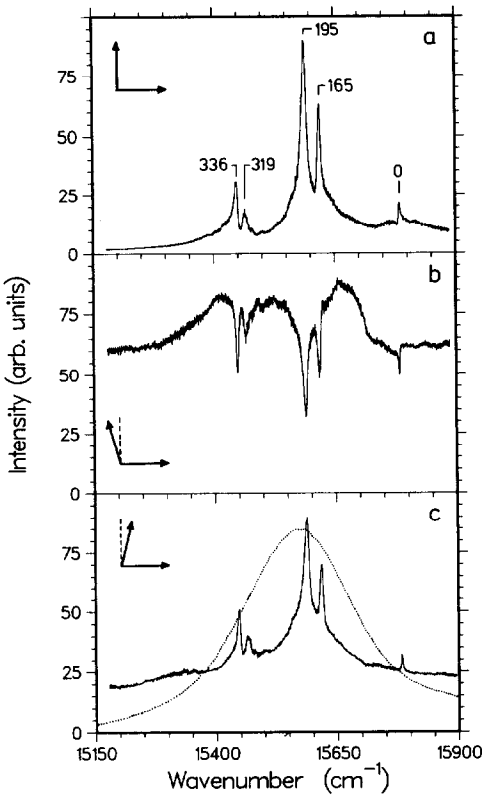

Fig. 5. Polarization spectra of type-II satellite holes burned into TPP in PMMA at $\nu_B = 15782\ cm^{-1}$ at a temperature of 10 K. (a) Polarizer and analyzer perfectly crossed, (b) polarizer rotated away from the analyzer mixing a negative background field to the signal, (c) polarizer rotated towards the analyzer mixing a positive background field to the signal.

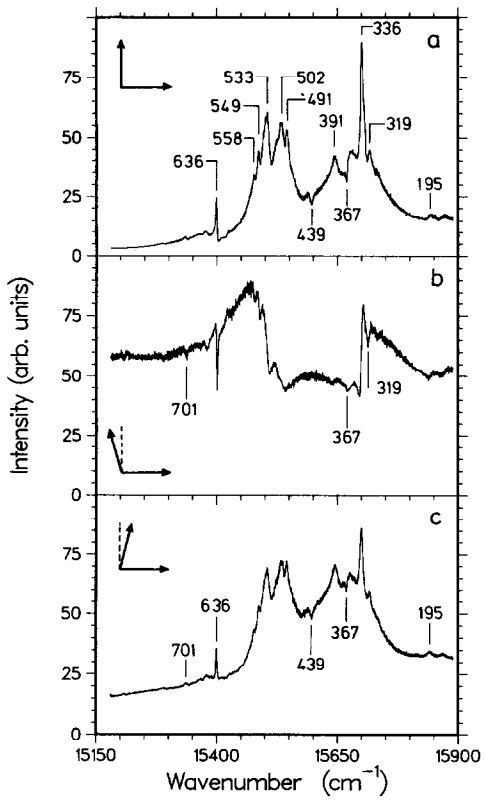

Fig. 6. Polarization spectra of type-II satellite holes burned into TPP in PMMA at $\nu_B = 16032\ cm^{-1}$ at a temperature of 10 K. Polarizer setting in (a)–(c) as in fig. 5.

very weak. Hence a shift of 250 cm^{-1} between successive hole-burning experiments is small enough to ensure sufficient overlap of the satellite-hole spectra.

The spectra in fig. 6 display many peaks corresponding to vibrational wavenumbers up to 701 cm^{-1}. The most prominent ones, which could all be reproduced very well, are labelled in fig. 6. An assignment is, however, not easy. The very sharp line at 636 cm^{-1} is due to a vibration with positive amplitude (parallel polarization), since it is inverted when a negative background is mixed to the signal (fig. 6b). The slightly dispersion-like character of this line in spectrum 6a indicates that it interferes with the wings of the broad bands with peaks between 491 and 558 cm^{-1}. This effect is reduced in fig. 6c due to the admixture of a positive background. The negative background added in spectrum 6b is not sufficient to invert the strong line at 336 cm^{-1}. Instead, this line appears with a dispersion-like shape, and the system of overlapping bands around 500 cm^{-1} shows a similar behavior. This indicates an underlying imaginary contribution to the background B which is most likely due to the contribution of holes burned into phonon sidebands. This can be reduced when hole-burning is performed with lower laser fluence, but in this case the broad bands around 500 cm^{-1} are rather weak. Two small but sharp negative lines at 367 and 439 cm^{-1} in figs. 6a and 6c are also difficult to assign since they are not inverted in fig. 6b as should be expected for perpendicularly polarized transitions.

The next hole-burning frequency, $\nu_{B3} = 16281$ cm^{-1}, falls close to the minimum of the absorption

spectrum (fig. 4). The hole spectra in fig. 7 reveal several sharp lines corresponding to vibrations with wavenumbers from 636 to 999 cm^{-1}. Three of these, at 763, 822 and 869 cm^{-1}, have a negative amplitude factor: they are inverted when a positive background field is mixed to the signal (fig. 7c), whereas all other lines are inverted with a negative background field applied (fig. 7b). It is interesting to note that each of these three perpendicularly polarized transitions is paired with a parallel polarized transition of similar intensity, namely at 746, 827 and 881 cm^{-1}. It could be speculated that these pairs correspond to vibrations that are degenerate in the ideal D_{4h} symmetry of the porphin skeleton. However, the degenerate vibrations belonging to the representation e_g in D_{4h} are out-of-plane vibrations. They should split into two vibrations with symmetry b_{2g} and b_{3g} in point group D_{2h}, the latter of which is symmetry forbidden for a transition to an electronic state of B_{3u} symmetry. Hence the near-degeneracies observed must be considered as accidental, a fact quite common with Raman spectra of porphins [19].

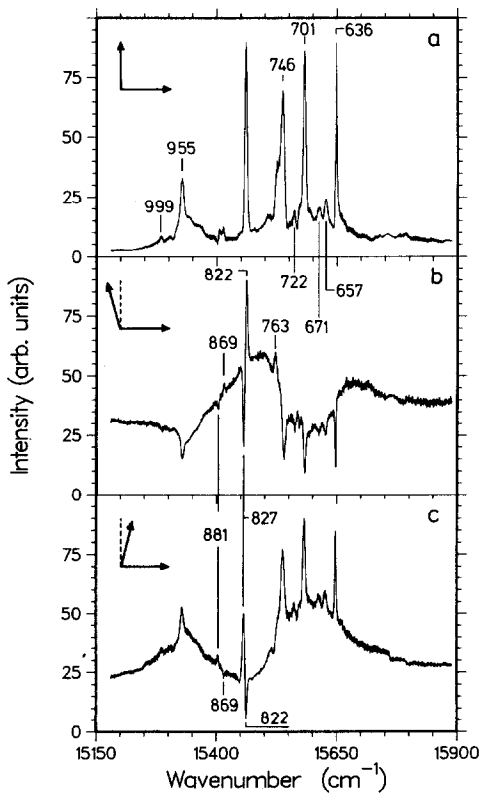

Fig. 7. Polarization spectra of type-II satellite holes burned into TPP in PMMA at $\nu_B = 16281$ cm^{-1} at a temperature of 10 K. Polarizer setting in (a)–(c) as in fig. 5.

When the hole-burning frequency is shifted by an additional increment of 250 cm^{-1} to higher energies, $\nu_{B4} = 16535$ cm^{-1}, the satellite of the 955 cm^{-1} vibration already visible in fig. 7 is brought to the center of the inhomogeneous distribution. With low hole-burning fluence it becomes by far the strongest satellite line in this spectral region (fig. 8a1). This vibration has a comparatively large Franck–Condon factor, which we noted already in the spectrum of type-I satellite holes in fig. 3. With higher hole-burning fluence additional weak lines appear (fig. 8a2), some of which did already appear in fig. 7. The new lines at 982, 1031, 1076 and 1122 cm^{-1} all have positive amplitude factors.

A quite different situation occurs for the next hole-burning frequency, $\nu_{B5} = 16785$ cm^{-1}. The polarization spectrum in fig. 9a displays four prominent peaks corresponding to vibrational wavenumbers of 1194, 1207, 1319 and 1356 cm^{-1}. All of these lines are inverted when a positive background field is mixed to the signal (see fig. 9c), hence the corresponding transitions are polarized perpendicular to the electronic origin. At about 1250 cm^{-1} the polarization spectrum with crossed polarizers, fig. 9a, displays low intensity with some structure. When a positive background field is mixed with the signal as in fig. 9c, these structures appear enhanced above the level of the baseline. Hence three vibronic transitions with transition moment parallel to the electronic transition can be assigned in this region at wavenumbers of 1227, 1246 and 1290 cm^{-1}.

The neighborhood of lines of similar intensity but with amplitude factors of opposite sign can make the spectra quite difficult to interpret. From the background-free spectra it is often not clear whether the maxima or the minima correspond to the line positions. This applies to the situation found with hole-burning at $\nu_{B6} = 17034$ cm^{-1} (see fig. 10). The polarization spectra obtained with negative (b) and positive (c) background field mixed to the signal are complementary: positive lines in (b) are negative lines in (c) and vice versa. Comparison of the baselines in (b) and (c) indicates that a broad back-

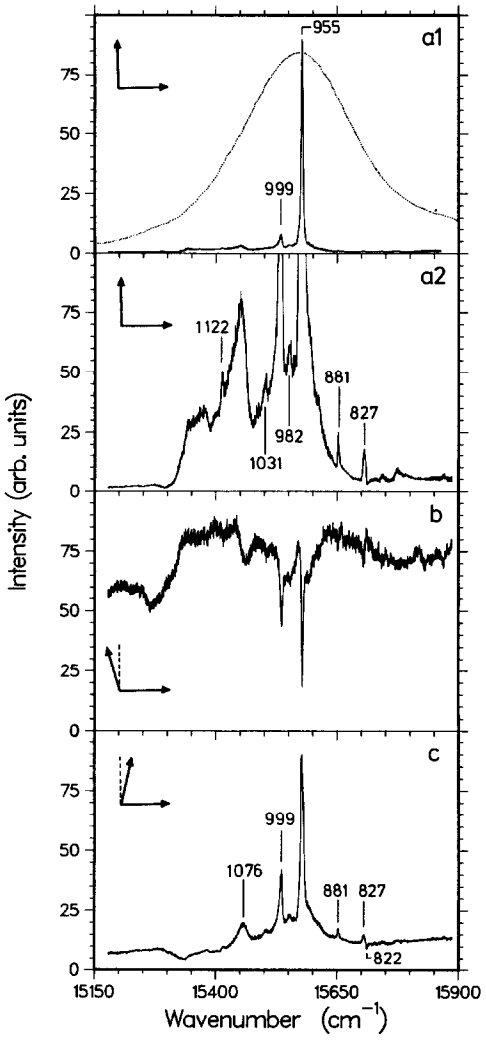

Fig. 8. Polarization spectra of type-II satellite holes burned into TPP in PMMA at $\nu_B = 16535$ cm^{-1} at a temperature of 10 K. Polarizer setting in (a)–(c) as in fig. 5. The spectra (a2)–(c) were obtained with a fluence for hole-burning seven times larger than for spectrum (a1).

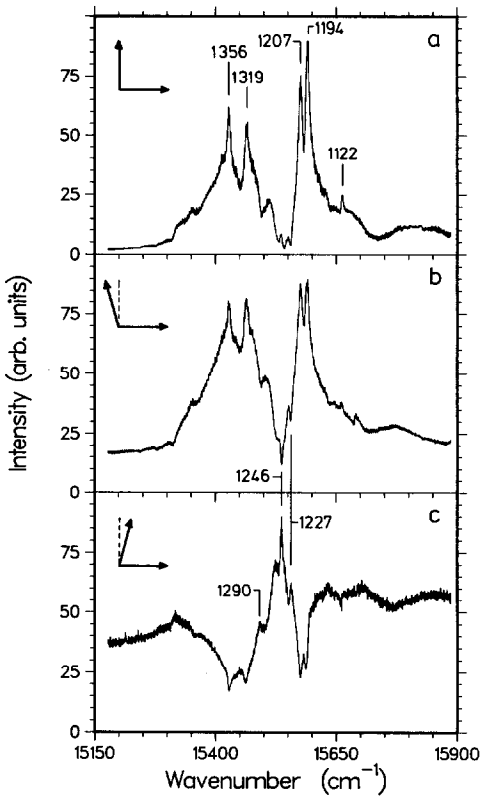

Fig. 9. Polarization spectra of type-II satellite holes burned into TPP in PMMA at $\nu_B = 16785$ cm^{-1} at a temperature of 10 K. Polarizer setting in (a)–(c) as in fig. 5.

ground with negative amplitude is underlying the whole spectrum. This is presumably due to burning into the phonon sidebands of the strong perpendicularly polarized transitions at 1319 and 1356 cm^{-1}. As a result the line at 1541 cm^{-1} in fig. 10a appears already inverted with crossed polarizers. Also, the peak at 1508 cm^{-1} in fig. 10a is not reproduced in the spectra with rotated polarizers, (b) and (c). This might indicate a distortion of the line due to interference with the phonon-sideband holes. Alternatively it could indicate the presence of a further line with negative amplitude, which could be responsible for the small peak at 1513 cm^{-1} in fig. 10b, but is not seen as negative peak in fig. 10c.

Hole-burning at $\nu_{B7} = 17281$ cm^{-1} projects vibronic states with vibrational wavenumbers between 1550 and 1850 cm^{-1} into the spectral window provided by the inhomogeneous band of the electronic origin. Many broad and interfering lines are obtained with crossed polarizers (see fig. 11a). A tentative assignment of line positions is possible from the spectra obtained with detuned polarizers. Extrapolation of the baseline (dotted lines in figs. 11b and 11c) indicates that a broad band with negative amplitude is underlying the spectrum. The lines appearing with

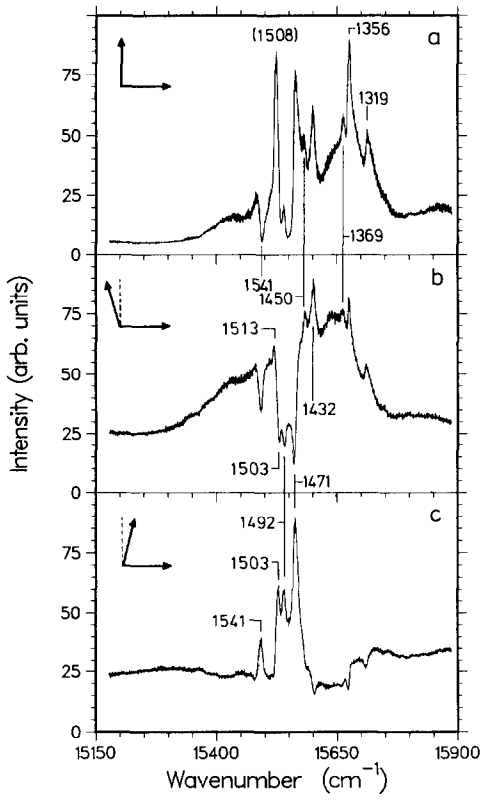

Fig. 10. Polarization spectra of type-II satellite holes burned into TPP in PMMA at $\nu_B = 17034$ cm^{-1} at a temperature of 10 K. Polarizer setting in (a)–(c) as in fig. 5.

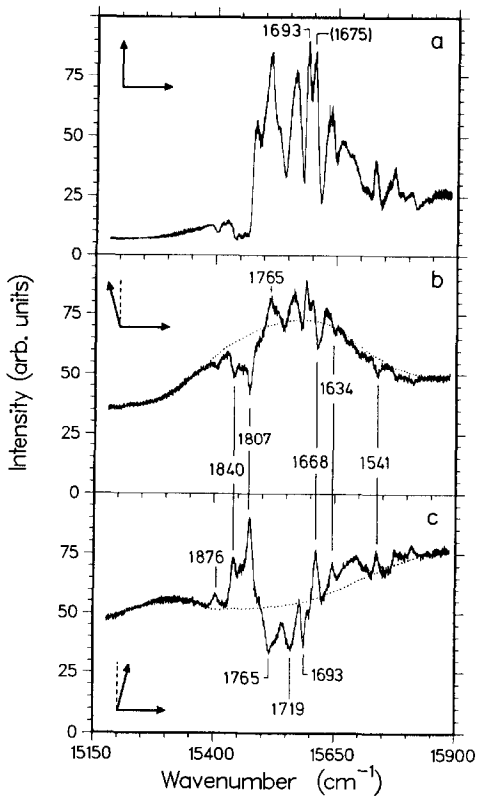

Fig. 11. Polarization spectra of type-II satellite holes burned into TPP in PMMA at $\nu_B = 17281$ cm^{-1} at a temperature of 10 K. Polarizer setting in (a)–(c) as in fig. 5.

opposite sign in the spectra (b) and (c) of fig. 11 have been labelled with their wavenumber differences to ν_{B7} and should correspond to vibrational line positions. No attempt of assignment has been made for hole-burning performed at even higher wavenumbers due to the increasing complexity of the spectra.

4. Discussion

4.1. Vibrational frequencies in S_1^x

The vibrational wavenumbers in the S_1^x state of TPP observed through hole-burning have been collected in table 2. They are compared to the corresponding wavenumbers observed in the fluorescence excitation spectra of TPP in a nitrobenzene Shpol'skii matrix [4], supersonic jet [5], and fluorescence spectra excited into the vibronic transitions of TPP in polystyrene [3]. Since all Franck–Condon factors are small it is likely that the potential surfaces of the electronic S_1^x state and the electronic ground state are very similar. Therefore, a comparison with the vibrational wavenumbers of the ground state obtained from resonance Raman spectra [19–21] seems also worthwhile.

All vibrations leading to strong lines in the satellite-hole spectra can also be found in the fluorescence excitation spectrum in Shpol'skii matrix, although not for all sites. The only exception is the line at 701 cm^{-1} which is, however, observed in the supersonic jet. On the other hand, the counterparts of the strong hole-burning satellites at 636, 1194, 1319 and 1471 cm^{-1} are missing in the supersonic-jet spectra. These might

Table 2
Vibrational wavenumbers of the electronic S_1^* state of TPP obtained from hole-burning (in PMMA), Shpol'skii spectra (in nitrobenzene), supersonic-jet, and fluorescence spectra in polystyrene. Vibrational wavenumbers of the electronic ground state obtained from resonance Raman spectra excited at different wavelengths are given for comparison. The symbols (+) and (−) give the sign of the amplitude of the lines in the polarization spectra and the polarization of the lines in the fluorescence spectra. (s): strong, (m): medium, (w): weak intensity

Hole-burning this work			Shpol'skii ref. [4]	Jet ref. [5]	Fluorescence ref. [3]		Resonance Raman		
							514.5 nm ref. [19]	457.9 nm ref. [20]	413.1 nm ref. [21]
165	+	s	161, 166	166	167	+	160		167
195	+	s	191–196	191	198	+	190	198	197
319	+	m	318, 319		320	+	318		
336	+	s	332–337	331			332	335	334
367	−?	w	?371–373		355	+			
391	+	m		388			404	410	
439	−?	w					431		441
491	+	m		487					
502	+	m	501, 502	507					500
533	+	m							533
549	+	m							
558	+	m							
636	+	s	638, 639				635	636	638
657	+	w		654					
671	+	w		672			671		674
701	+	s		700					
722	+	w		718					
746	+	m	748–755	?741					
763	−	m		758					
822	−	s	818–821	818					
827	+	s		824	825	+	826	828	833
869	−	w					868		
881	+	w					881		886
955	+	s	952–954	950	955	+	961	961	962
982	+	w	972	986	969	−			
999	+	m	996–1000	1000	1001	+	1000	1003	1004
1031	+	w							1030
1076	+	m	1064–1070		1080	+	1076	1084	1076
1122	+	w	1118–1119		1124	+	1135		1135
1194	−	s	1190–1193		1195	−			
1207	−	s	1203–1207	1211	1207	−	1204		
1227	+	s	1229–1232	1241	1227	+	1239	1234	1234
1246	+	s	1253–1258	1258	1248	+	1277		
1290	+	m			1260	+			
1319	−	s	1315		1321	−	1327	1330	1327
1356	−	s	1354–1364	1365	1358	−	1358		1357
1369	−	w					1372		1383
1432	−	m	1424–1435		1433	−	1437		1438
1450	−	m	1458		1447	+	1456		
1471	+	s	1462		1471	+	1488		1485
1492	+	s	1499–1501				1497	1501	1499
1503	+	s	1504, 1505	1511	1507	+	1551	1553	1550
1513	−?	m	1511, 1514	1515					
1541	+	m	1541–1545		1543	+			
1634	+	m							

(continued on next page)

Table 2 (continued)

Hole-burning this work			Shpol'skii ref. [4]	Jet ref. [5]	Fluorescence ref. [3]		Resonance Raman		
							514.5 nm ref. [19]	457.9 nm ref. [20]	413.1 nm ref. [21]
1668	+	m			1675	+			
1682	–	w							
1693	–	m							
1719	–	m		1710	1703	+			
1765	–	m		1752					
1807	+	m							
1840	+	m							
1876	+	w		1874					

arise from configurations which are stabilized in the rigid matrix but are unlikely to occur in the isolated molecule. E.g., in rigid matrix the phenyl groups could be fixed at various torsional angles in such a way that the inversion symmetry is broken. In the Shpol'skii matrix two groups of sites are observed separated by about 500 cm^{-1} which have been assigned to conformers with different torsion angles of the phenyl groups [4]. Some vibrational transitions might be stronger in some of these conformers than in others, explaining the fact that not all vibrations are observed for all sites. In PMMA a continuous distribution of torsional conformers is possible. The progressions in a 20 cm^{-1} mode assigned to phenyl-ring torsion seen in the supersonic jet are absent from the hole-burning spectra. This might indicate that torsion of the phenyl rings is frozen in PMMA matrices, or that the Franck–Condon factors of these transitions are much smaller in PMMA such that these transitions are hidden under the phonon sidebands.

A fluorescence technique has been used by Bykovskaya et al. [3] to measure the vibrational frequencies of the S_1^x state of TPP in polystyrene matrix at 4.2 K. With laser irradiation into the region of overlapping vibronic bands they selectively excited several subensembles – one for each vibration – in the same manner as we did for hole-burning of type-II satellite holes. These subensembles are then monitored by their fluorescence on the electronic origin transition. The degree of polarization of the fluorescence is positive (negative) for vibronic transitions polarized parallel (perpendicular) to the electronic origin. In terms of the symmetry assignment of the vibrations this information is equivalent to the sign of amplitudes in the polarization spectra. A comparison of our vibrational wavenumbers and sign factors shows excellent agreement [#2] with those of ref. [3]. The only larger discrepancy is that we find a line at 1290 cm^{-1} while in ref. [3] a line at 1260 cm^{-1} is found. The sign factors for the vibrations at 969, 1447 and 1703 cm^{-1} in ref. [3] differ from those found in the hole-burning spectra for the corresponding lines. However, these assignments were only tentative in ref. [3] due to the background of adjacent lines. Interestingly, the sharp lines between 400 and 800 cm^{-1} were not found with the fluorescence method.

A comparison of the vibrational wavenumbers of the electronic excited S_1^x state with those of the electronic ground state S_0, obtained from resonance Raman spectra [19–21], reveals a large number of close similarities. Obviously the potential surfaces of both states are very similar leading to only very small changes in the vibrational frequencies. Hence the assignment of the vibrational wavenumbers of the ground state given in ref. [21] can be transferred to those of the S_1^x state.

4.2. Correlation of the inhomogeneous distributions

A comparison of the widths of resonant holes and satellite holes yields information on the degree of correlation between the inhomogeneous distributions of vibronic absorption bands within the same electronic state. In the limit of perfect correlation the

[#2] Our assignment was not influenced by that given in ref. [3] since we received a copy of this paper only when our assignment given in table 2 was completed.

difference Δ between the width of the satellite hole and the mean width of the two corresponding resonant holes should be zero. The widths of all satellite holes with reasonable intensity can easily be determined, and also the width of the resonant hole in the electronic origin. The widths of the resonant holes in the vibronic states are, however, difficult to obtain. The reason is that the vibronic bands strongly overlap and that irradiation into the region of these overlapping vibronic bands produces a superposition of many resonant holes. The weights of the various vibronic states involved can be estimated from the intensities of the corresponding type-II satellite holes. Only if a single satellite has dominant intensity, the resonant hole can be assigned to the corresponding vibronic state. The line at $\Delta\nu = 955\ \mathrm{cm}^{-1}$ in fig. 8 is the best example. Table 3 lists a few linewidths of resonant and satellite holes. Spectra produced with low fluence for hole-burning have been used in all cases to reduce line broadening through saturation of the photochemical reaction. The widths of resonant lines in parentheses cannot be assigned to a single transition but refer to a goup of close-lying transitions. All satellite holes are larger than the resonant holes indicating that correlation within the inhomogeneous distribution is not perfect. Imperfect correlation is described by a two-dimensional distribution function $g(x, y)$ where x and y are the spectral shifts within the inhomogeneous distributions of the $|a\rangle \rightarrow |b\rangle$ transition and the $|a\rangle \rightarrow |c\rangle$ transition. The two-dimensional distribution function can be modelled as the product of two Gaussian distributions of dependent [22] or independent [23] variables. However, an analytic function is not needed here. The variances

$$\sigma_x = \sqrt{\langle xx \rangle} \quad \text{and} \quad \sigma_y = \sqrt{\langle yy \rangle} \tag{2}$$

can serve as a measure of the widths of the inhomogeneous distributions for the two vibronic transitions. In the same way the width of the inhomogeneous distribution for the vibrational frequency is characterized by

$$\sigma_v = \sqrt{\langle (x-y)^2 \rangle}\,. \tag{3}$$

The correlation coefficient, defined as $r = \langle xy \rangle / (\sigma_x \sigma_y)$ is related to these variances by

$$1 - r = \frac{\sigma_v^2 - (\sigma_x - \sigma_y)^2}{2\sigma_x \sigma_y} \leqslant \frac{\sigma_v^2}{2\sigma_x^2}\,. \tag{4}$$

In the second step it was assumed that σ_x is smaller than σ_y. Within the two-dimensional Gaussian model with the independent variables $\xi = (x+y)/\sqrt{2}$ and $\eta = (x-y)/\sqrt{2}$ the correlation loss $1-r$ is exactly given by the rhs of eq. (4). The inhomogeneous width (fwhm) of the electronic origin band of TPP in PMMA at 10 K is 280 cm^{-1}. This width can be assigned to σ_x, e.g., for a Gaussian lineshape we have $\sigma_x \sqrt{8 \ln 2} = 280\ \mathrm{cm}^{-1}$. The lineshape of the satellite hole is the square modulus of the convolution of a complex Lorentzian with width $B_L = 2(\Gamma_{ab} + \Gamma_{ac})$ and the vibrational inhomogeneous distribution function $g_v(x-y)$. Hence σ_v must in general be found by deconvolution, e.g., assuming a Gaussian for $g_v(x-y)$. However, the ratio of the widths of the satellite hole and the inhomogeneous absorption band is always an upper limit to the ratio σ_v/σ_x. With these we obtain the upper limits to the correlation loss $(1-r)$ given in table 3. These values range over almost two orders of magnitude. The correlation coefficient itself is, however, close to unity in all cases.

Table 3
Linewidths (fwhm) of the resonant hole and the satellite holes for several vibronic states in the electronic S_1^x state of TPP in PMMA. ν: vibrational wavenumber, Δ: width of satellite hole minus mean of the resonant holewidths. $1-r$: upper limit of correlation loss.

ν (cm^{-1})	Resonant hole	Satellite hole	Δ	$(1-r)\times 10^5$
0	1.0			
165		8.2		43
195	(1.2)	13.8	(12.7)	121
336	3.2	6.4	4.3	26
636		2.2		3
701		6.8		29
746		11.0		77
822		4.0		10
827		3.6		8
955	2.8	4.4	2.5	12
999		5.4		19
1194	(6.0)	9.0	5.5	52
1207	(6.0)	10.8	7.3	74
1319		12.4		98
1356		15.8		159
1471	(5.6)	14.2	10.9	129
1541	(5.6)	12.0	8.7	92

5. Summary

The results of the present investigation can be summarized as follows:

(1) Polarization spectroscopy of vibronic satellite holes has been applied to the molecule meso-tetraphenylporphin in a PMMA matrix at 10 K. The absorption spectrum of this molecule in the region of the first electronic transition consists of only two broad bands. With the hole-burning method a line-narrowed spectrum of this electronic transition with more than 50 resolved vibronic lines could be obtained.

(2) Two variants of satellite hole-burning have been investigated. In the first, laser irradiation into the electronic origin band produces the spectral hole, and the vibrational satellite holes are obtained in a single scan over the absorption spectrum. In the second, hole-burning is performed in the region of overlapping vibronic bands and the satellite holes corresponding to these overlapping vibronic bands are detected by a scan over the electronic origin band. Although in the latter method repeated experiments with several hole-burning frequencies are necessary to obtain a complete spectrum, it yields far better spectra when the Franck–Condon factor of the electronic origin is larger than that of the vibronic transitions.

(3) The vibrational wavenumbers and polarizations found with hole-burning for the first electronic excited singlet state of TPP in PMMA are in good agreement with corresponding literature data obtained with fluorescence methods in the supersonic jet, the crystalline Shpol'skii host nitrobenzene, and the hydrocarbon matrix polystyrene.

(4) The analysis of the linewidths of resonant and satellite holes revealed that the inhomogeneous distributions of the vibronic transitions are not perfectly correlated with the inhomogeneous distribution of the electronic origin. Inhomogeneous broadening of the vibrational transitions within the first excited electronic singlet state of TPP with widths up to about 10 cm^{-1} is found. This indicates that the vibrational frequencies of these transitions are sensitive to the environment.

Acknowledgement

The author is greatly indebted to Professor F.P. Schäfer for generous support of this work, and to Dr. T. Jovin for the loan of a Soleil–Babinet compensator. The MMA monomer was purified by D. Ouw, and the PMMA samples optically polished by W. Sauermann. This work was supported by the Deutsche Forschungsgemeinschaft through the Leibniz-Prize program and project SFB 93 (Photochemie mit Lasern).

References

[1] B. Dick, Chem. Phys. 136 (1989) 413.
[2] B. Dick, Chem. Phys. Letters 143 (1988) 186.
[3] L.A. Bykovskaya, R.I. Personov and Yu.V. Romanovskii, Zh. Prikl. Spektroskopiya 31 (1979) 910.
[4] R. Tamkivi, I. Renge and R. Avarmaa, Chem. Phys. Letters 103 (1983) 103.
[5] U. Even, J. Magen, J. Jortner, J. Friedman and H. Levanon, J. Chem. Phys. 77 (1982) 4374.
[6] B. Dick, in preparation.
[7] A.A. Gorovskii and J. Kikas, Opt. Commun. 21 (1977) 272.
[8] S.J. Silvers and A. Tulinsky, J. Am. Chem. Soc. 89 (1967) 3331.
[9] M. Gouterman, J. Mol. Spectry. 6 (1961) 138.
[10] B. Norden and Å. Davidsson, Chem. Phys. Letters 37 (1976) 433.
[11] N. Fischer, E.V. Goldammer and J. Pelzl, J. Mol. Struct. 56 (1979) 95.
[12] H.P.H. Thijssen, A.I.M. Dicker and S. Völker, Chem. Phys. Letters 92 (1982) 7.
[13] B.M. Kharlamov, C.A. Bykovskaya and R.I. Personov, Chem. Phys. Letters 50 (1977) 407.
[14] B.L. Feary, F.P. Carter and G.J. Small, J. Phys. Chem. 87 (1983) 3590.
[15] A.D. Adler, F.R. Longo, J.D. Finarelli, J. Goldmacher, J. Assour and L. Korsakoff, J. Org. Chem. 32 (1967) 476.
[16] H.P.H. Thijssen and S. Völker, J. Chem. Phys. 85 (1986) 785.
[17] H.P.H. Thijssen and S. Völker, Chem. Phys. Letters 120 (1985) 496.
[18] H.P.H. Thijssen, R. van den Berg and S. Völker, J. Phys. (Paris) 46 (1985) C7-363; Chem. Phys. Letters 120 (1985) 503.
[19] R. Mendelsohn, S. Sunder and H.J. Bernstein, J. Raman Spectry. 3 (1975) 303.
[20] K. Shoji, Y. Kobayashi and K. Itoh, Chem. Phys. Letters 102 (1983) 179.
[21] P. Stein, A. Ulman and T.G. Spiro, J. Phys. Chem. 88 (1984) 369.
[22] J. Friedrich and D. Haarer, J. Chem. Phys. 78 (1983) 1612.
[23] B. Dick and R.M. Hochstrasser, J. Chem. Phys. 78 (1983) 3398.